CHAPTER-5

QUANTITATIVE LANDSCAPE ANALYSIS OF THE NSF ZONE

Quantitative analysis of landscape through various geomorphic indices is useful for geomorphometric characterization of landforms and evaluating the degree of active tectonics in a given area (Strahler, 1952; Bull and McFadden, 1977; Keller et al. 2000; Keller and Pinter, 2002). Further, area undergoing active tectonics commonly has topography that can assist in identifying different geomorphic or structural segments and estimating the potentially most active segments (Azor et al., 2002, Font et al., 2010). As it is not possible to define any parameter which would be able to isolate systematically the tectonic impact in an area. Hence, the geomorphic indices of active tectonics combined with morphotectonic analyses of the area have been proved useful in ascertaining the level of tectonic uplift and in indentifying segments undergoing rapid tectonic uplift. Data on geomorphic indices were generated using Remote Sensing data and GIS software (Troiani, 2007). Using Shuttle Radar Topography Mission (SRTM) data and GIS techniques is a effective, fast, inexpensive and precise way for carrying out morphostructural analyses (Farr and Kobrick, 2000; Grohmann, 2004; 2007).

A detailed quantitative landscape analysis of the NSF zone was carried out with an objective to know the relative level of Late Quaternary tectonic activity along the length of the NSF. The study comprises terrain analysis from DEM and its derivatives, followed by calculation of geomorphic indices including mountain front sinuosity (Smf), longitudinal profiles, hypsometric curves and hypsometric integral (HI), asymmetry factor (AF), stream length gradient index (SL-Index) and sinuosity (S).

TERRAIN ANALYSIS

Digital Elevation Model (DEM) Analysis

Digital Elevation data are a key element in modeling landscape in fault zones (Menges, 1990; Duncan et al. 2003, Ganas et al. 2005). Digital Elevation Model was analyzed using SRTM data (90 m) as it is inexpensive, easily accessible, reliable and effective for geomorphic analysis of a given area over the regional scale. DEM records the topographic expression of an area from which different computer algorithms like slope, aspect and shaded relief can be extracted. The tonal variation property of the DEM is useful in understanding the topography and structural features of a region. Various geomorphic features have been observed from sharp changes in tone that are related to corresponding changes in topographic relief. The distribution of spectral brightness from dark brown to pale green tone is in accordance with the terrain relief (Fig.4.1). A continuous ENE-WSW trending linear dark yellow to brown boundary indicates the location of NSF scarp which is easily matched with long breaks in slope (Fig. 4.1). In front of the scarp, the highly rugged relatively dark green tonal surface represents alluvial plain which is superimposed by north flowing parallel drainages (Fig. 4.1). It is clearly visible that the drainages of segment II are deeply incised compared to the drainages of other three segments. The prominent straight course of the Karjan River and Madhumati River near the scarp is seen which may be attributed to the segment bounding fault Karjan Fault and Madhumati fault respectively. The other prominent ENE-WSW trending linear feature visible in the western part with light green tone is the palaeobank of Narmada River (Fig. 4.1).

Slope Analysis

Abrupt change in slope across the landscape is one of the indications of active faulting (Sanders and Selmmons, 1996; Hooper et al. 2003). The lineaments as seen in the slope maps may represent fault scarp localities (Ganas et al. 2005). It is observed that in Segment I, II and III, the slope break of 19.41 degrees exists in the vicinity of range front scarp manifested by yellow-orange to pale green tonal transition (Fig. 5.1). In the segment IV the slope break goes down to 5.4 degrees as shown by yellow to pale green tonal transition (Fig. 5.1). This featurealso correlates well with elevation data wherein, the tonal transition from yellow-brown to dark green is seen in the DEM analysis (Fig. 5.1). The other feature of good significance is the high degree of slope change (3-4 degrees) across the channel reach in alluvium. The ravine surfaces occurring all along the Narmada River also shows visible change in slope (2-3 degrees). Hence, it can be noted that the rivers in the NSF zone are incisive rather than aggradational. The responsible factor for this is neotectonics as observed in the vicinity of the fault. Therefore, active tectonics along NSF is identified as major factor in producing linear slope breaks and incised channels.

Aspect Analysis

Aspect map is the second derivative of the elevation data as it uses slope data to calculate aspect of the given pixels which is generated through 3D Analyst tool in ArcGIS. Aspect identifies the steepest down slope direction for each cell compared to its neighboring cell for the entire region. Aspect is measured clockwise in degrees from 0 to 360. Flat area having no down slope direction is given a value of -1. On the aspect map, in the eastern part of figure majority of pixels in the vicinity of scarpline have dark pink tone indicating northward slope direction. The same pixel tone found in the western part of of the figure is expressed as linear ENE-WSW trending steep, north facing linear feature (Fig. 5.2). This pattern matches with the interpretations of DEM and slope map (Fig. 5.1, 5.2). In the upland area, southerly dipping sky blue colored pixels are found which verify the southward tilting of the basaltic flows which relates to tectonic movements along the NSF (Fig. 5.2).

Shaded Relief

Shaded relief maps are useful to infer the geometry of footwall block along the strike of the major faults and it is also used to extract and study drainage patterns. In this algorithm, the illumination value for each cell is calculated by setting a position for hypothetical source of illumination (in degrees, {0-360}) and calculating illumination value for each cell in relation to its neighboring cell. These values ranges from 0–255 (dark to light shades in gray scale), the 0 value is assigned to the cell which is not illuminated and it increases according to illumination conditions. Different views of illumination source can be decided on the basis of DEM resolution and tectonic setting of the area. It greatly enhances the visualization of topography. Also shaded relief map can be used in the background for the overlay of other vector or raster layers. The shaded relief map was generated from 3D analyst tool of ArcGIS with 170^0 azimuth angle of light source and 30^0 altitude angle above the horizon. A steep range front scarp is clearly visualized and existence of highly incised transverse river valleys are also clearly seen (Fig. 5.3). Maximum steepness with 0 hillshade value is seen in the Segment I and II.

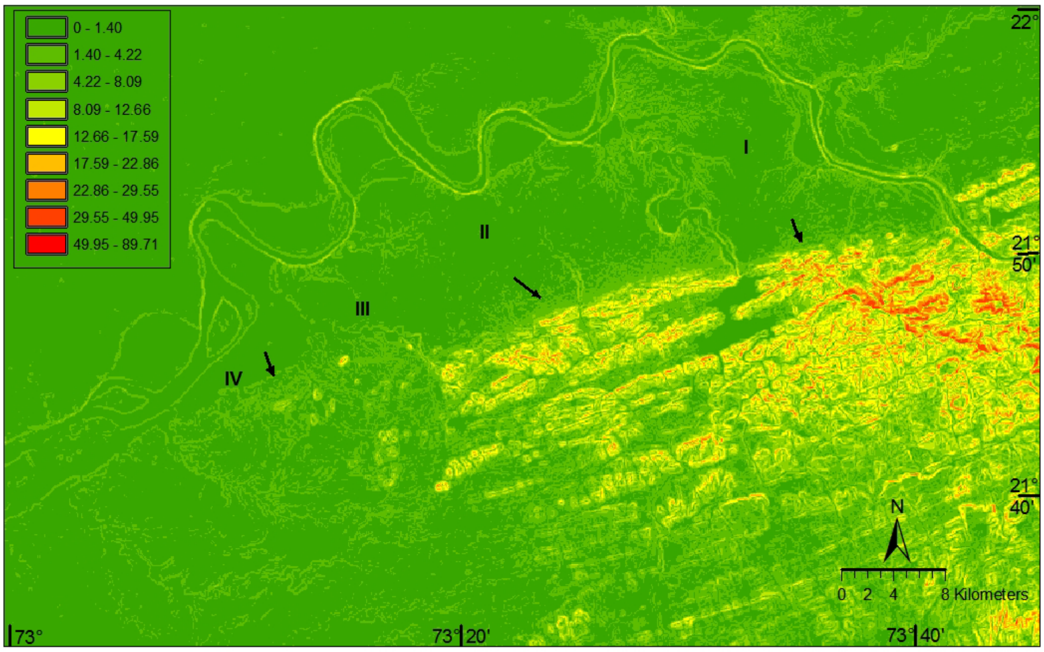

Figure 5.1 Slope map of the study area. Slope values are in degrees. Arrows indicate the steep northward slopes formed in alluvial plain close to the scarps. Note the north flowing drainages meeting the Narmada River and erosional gullies (ravines) with high degree of slope suggesting fluvial dissection.

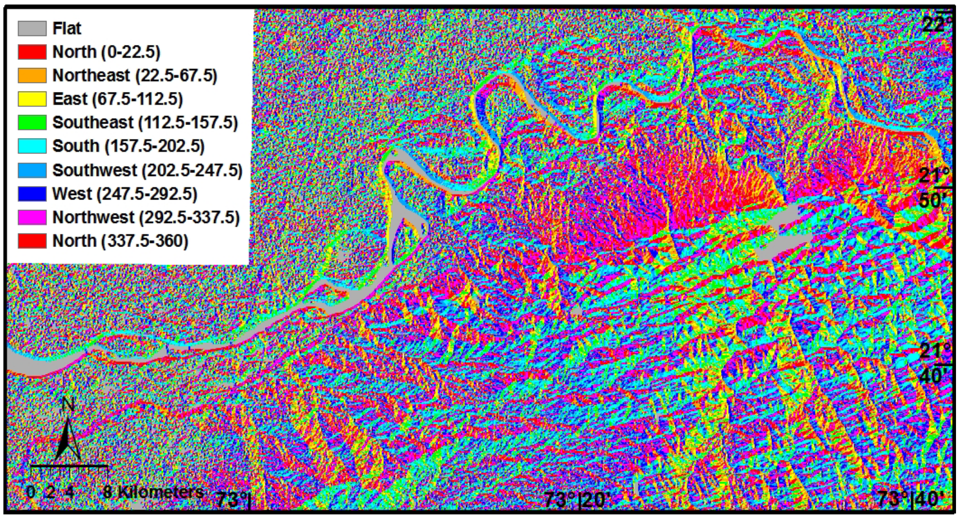

Figure 5.2 Aspect map of the study area. Note the dark pink colored pixels along the NSF zone indicating northward slope.

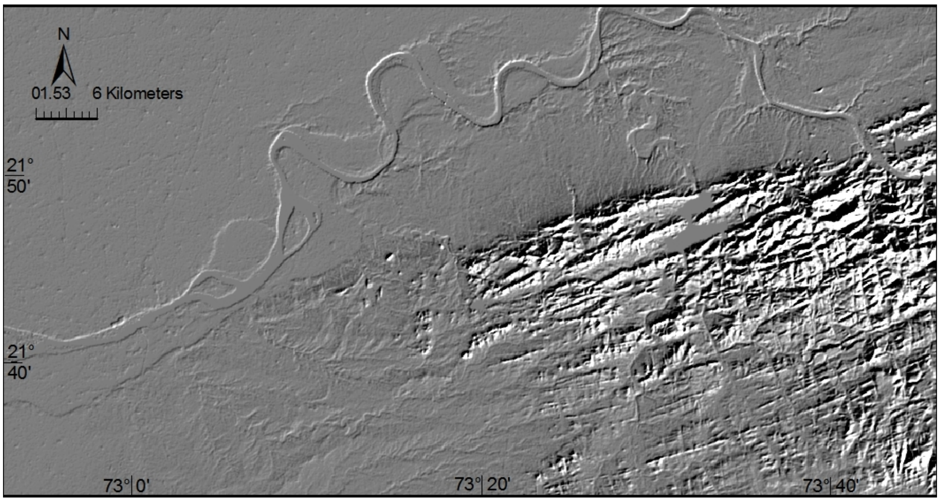

Figure 5.3 Shaded relief map of the study area.

Longitudinal river profiles

Longitudinal profiles stream channels results from the interactions between fluvial incision, lithology, tectonics and base level changes (Larue, 2008) and it effectively shows the balance between erosion and uplift (Molin and Fubelli, 2005; Schumm et al., 2000; Keller and Pinter, 2002; Menéndez et al., 2008; Bull, 2009a). Longitudinal profiles of the trunk streams of the ten drainage basins astriding the NSF in the study area were drawn from the survey of India topographic maps of 1:50,000 scale (Fig. 5.4). The change in the morphology of the profiles correlates with the sharp physiographic contrast across the NSF zone. Most of the streams exhibit knick points in the resistant rocks of the uplands (Deccan basalts and Tertiary rocks) and steep gradient with straight reaches in non-resistant alluvial lithology (Fig. 5.4). The knick points are located close to the intersection of channels with the NSF. Accordingly, tectonic uplift of block at the upslope is attributed to neotectonic activity along NSF.

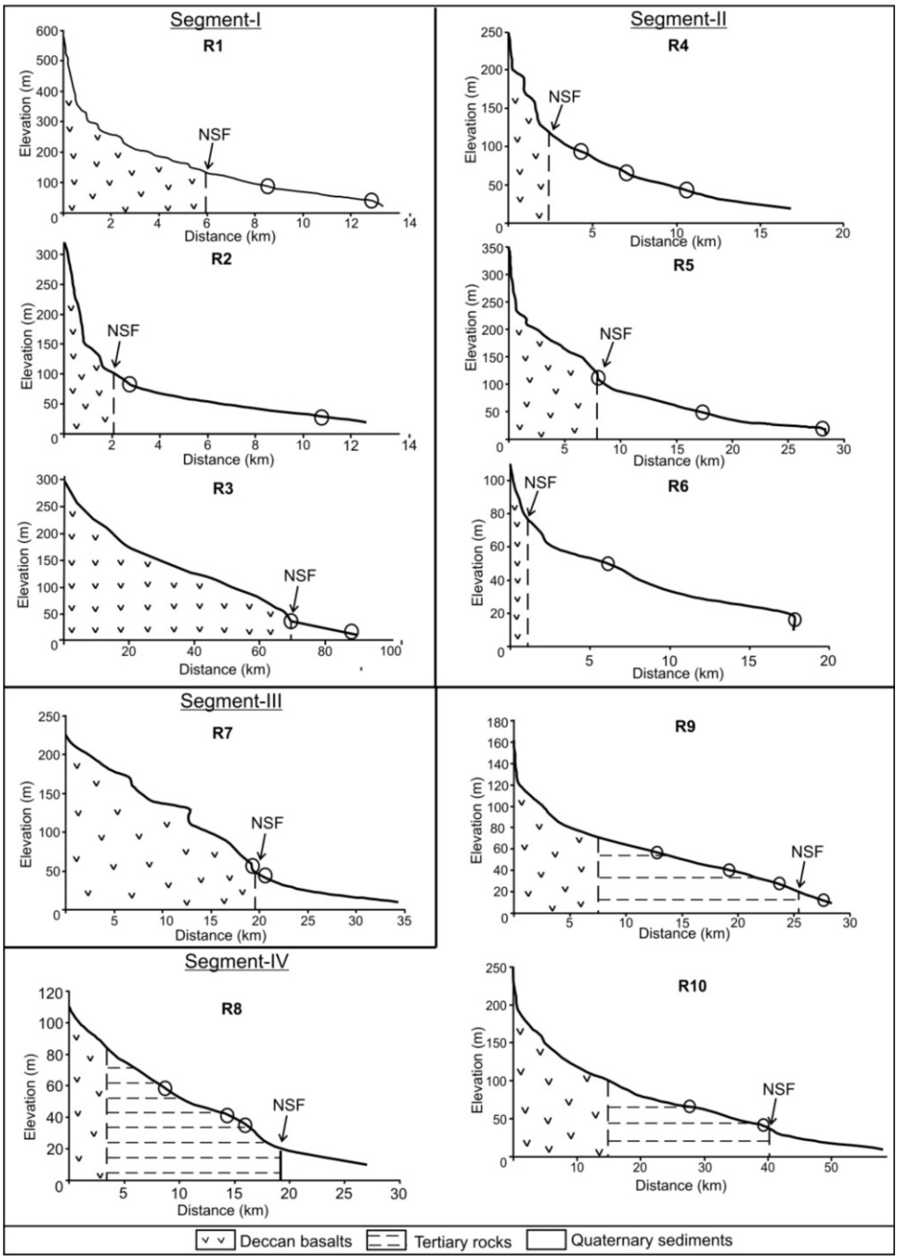

Figure 5.4 Longitudinal river profiles of the trunk streams of drainage basins R1 to R10. Note the steepened reach of the profiles in the vicinity of the NSF. Circles show the locations of anomalous high values of Stream Length Gradient index (SL index) shown in Table 5.1.

Pronounced variations in the morphology of the channel profiles are observed in different segments of the NSF (Fig. 5.4). Profiles of R1, R2 and R3 in Segment I show steep gradients in upland reach which is contrasted with the graded nevertheless steeper profile in the alluvial reach. The profile of R3 (Karjan River) shows higher degree of grading as it is a higher order stream that also forms the largest tributary drainage basin in the area. The profiles show good correspondence with the less incision in Segment I compared to other segments to the west. The profiles of rivers (R4 to R7) in Segment II show distinct convex up morphology in the alluvial zone. The convex up part of the profile is closer to the interface between the upland rocks and alluvium marking the NSF.

This suggests rejuvenation of this segment in response to neotectonic activity along the NSF. This is supported by the highest degree of elevation and incision (40 m) observed in this segment as described earlier in Chapter 4. Madhumati River in alluvial reach flows along a transverse fault delimiting Segment II in the west. It follows a NW course after emerging from the uplands instead of flowing towards north. In Segment IV, longitudinal profiles of R8 to R10 show convex up morphology in the Tertiary rocks suggesting neotectonic rejuvenation of the area due to movements along the NSF (Fig. 5.4). The shorter extent of rivers in the alluvial plain shows steep gradients confirming neotectonic activity along the NSF. Variations in morphology of longitudinal profiles of various rivers in different segments of the NSF zone compliment the geomorphic and drainage characteristics suggesting spatially variable intensity of neotectonic activity along the length of the NSF. Highest magnitude of neotectonic activity in segment II is inferred.

GEOMORPHIC INDICES

Five geomorphic indices which are reliable indicators of active tectonics (Keller and Pinter, 2002) were calculated including mountain front sinuosity (S_{mf}), hypsometric curves and hypsometric integral (HI), drainage basin asymmetry (AF), stream length gradient index (SL index) and sinuosity (S).

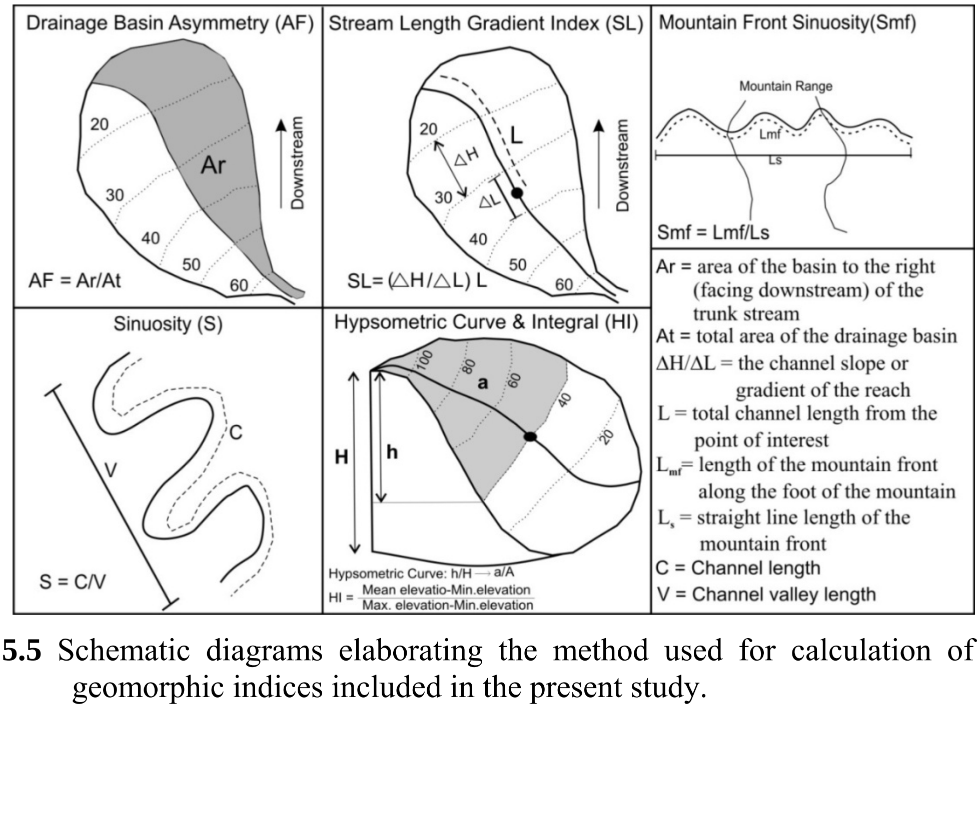

Figure 5.5 Schematic diagrams elaborating the method used for calculation of various geomorphic indices included in the present study.

Mountain front sinuosity

Mountain front sinuosity is defined as the ratio between the length along the foot of the mountain front and the straight line length approximately parallel to the mountain front (Bull and McFadden 1977, Bull 1978; Keller and Pinter, 2002). Mountain front sinuosity is an index that reflects the balance between erosional forces that tend to cut embayments into a mountain front and tectonic forces that tend to produce a straight mountain fronts associated with active tectonics and uplift. Those mountain front associated with active tectonics are relatively straight with low values of S_{mf} (~ 1). Low S_{mf} value indicates youthfulness of mountain fronts due continued neotectonic activity (Bull and MacFadden, 1977). If the rate of uplift is reduced, then erosional processes carve a more irregular mountain front and the S_{mf} value will increase. The mathematical derivation of Mountain Front Sinuosity is;

$$S_{mf} = L_{mf} / L_s$$

Where S_{mf} is the mountain front sinuosity, L_{mf} is the length of the mountain front along the foot of the mountain, and L_s is the straight line length of the mountain front.

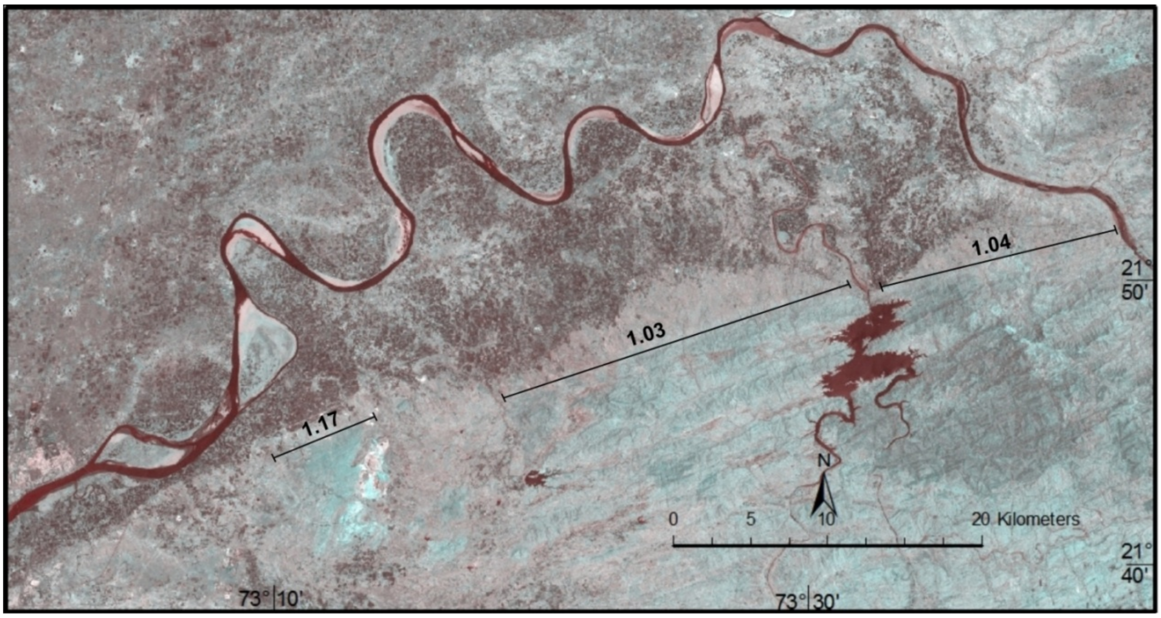

Figure 5.6 Landsat Thematic Mapper (TM) image overlapped over the shaded relief map. The arrow shows the prominent northward slope of the alluvial terrain near the NSF. Dark lines indicate the mountains fronts studied with Smf values.

The mountain front sinuosity is measured for three segments (Fig. 5.6) from Landsat ETM+ image. The S_{mf} values obtained for segment-I (1.04), II (1.03) and IV (1.17) are very low, suggesting tectonically active mountain fronts. The difference in S_{mf} values correspond to the lateral variation in magnitude of tectonic activity along NSF which is consistent with the results of terrain and drainage analysis.

Hypsometric curve and Hypsometric integral

Hypsometry is the relative portion of an area of different elevation within a region (Strahler, 1952). The calculation of hypsometric curve and hypsometric integral has become vital with the advent of DEM (Gardner et al., 1990). Hypsometric curve is a very useful geomorphic index to determine the stage of development of watersheds. The curve is created by plotting proportion of total basin height (h/H) against the proportion of total basin area (a/A). A useful attribute of the hypsometric curve is that drainage basins of different sizes can be compared with each other because area and elevation are plotted as function of total area and total elevation. The ratios of h/H and a/A calculated with the help of ArcMap for individual drainage basins using contour map. The shape of the curve is related to the degree of dissection of the basin. Convex hypsometric curves characterize relatively "young" regions, S-shaped characterize moderately eroded regions and concave hypsometric curves indicate relatively "old" regions. It is clearly visible in Fig.5.7 that the shape of the curves varies for different segments from east to west whereas the basins of same segment have nearly similar shape of hypsometric curve. All over the hypsometric curves have sigmoidal shape that suggests moderately eroded landscape and the early mature stage of cycle of fluvial erosion.

The hypsometric integral is defined as the area under the hypsometric curve. One way to calculate the integral for a given curve is as follow (Pike and Wilson, 1971; Mayer, 1990; Keller and Pinter, 2002).

$$\frac{\text{Mean elevation} - \text{Minimum elevation}}{\text{Maximum Elevation} - \text{Minimum elevation}}$$

The relationship between the hypsometric integral and degree of dissection permits its use as an indicator of landscape's stage in the cycle of erosion. According to the development stage of watersheds: (i) the curve of young immature watershed offers a convex form and high integral value (> 0.5) (ii) in the mature case the curve takes a concave shape upstream, convex shape downstream (in case of homogenous lithology) and an integral lower than the previous case (< 0.5) (Strahler, 1957; Delcaillau et al. 1998; Keller and Pinter, 2002). The hypsometric curves shown in Fig. 5.7 show dominantly concave shapes and appear similar in the first instance. However, distinct convex up tendency of the curves can be seen at least in one basin in each segment. This is observed in case of R1 in Segment-I, R5 in Segment-II and R9 in Segment-IV (Fig. 5.7). The convex part of the curves coincides with the NSF zone indicating slightly younger stage of erosion in the vicinity of the NSF. The mean values of HI of segments I, II and IV are, 0.42, 0.45 and 0.43 respectively. Among these segments, the drainage basins of Segment II have highest mean HI value which is also reflected by convex hypsometric curve more prominently seen in case of drainage basin R5 which is located in central part of the segment (Fig. 5.7). Overall, the curves in conjunction with moderate HI values suggest dissected landscape, approaching equilibrium phase.

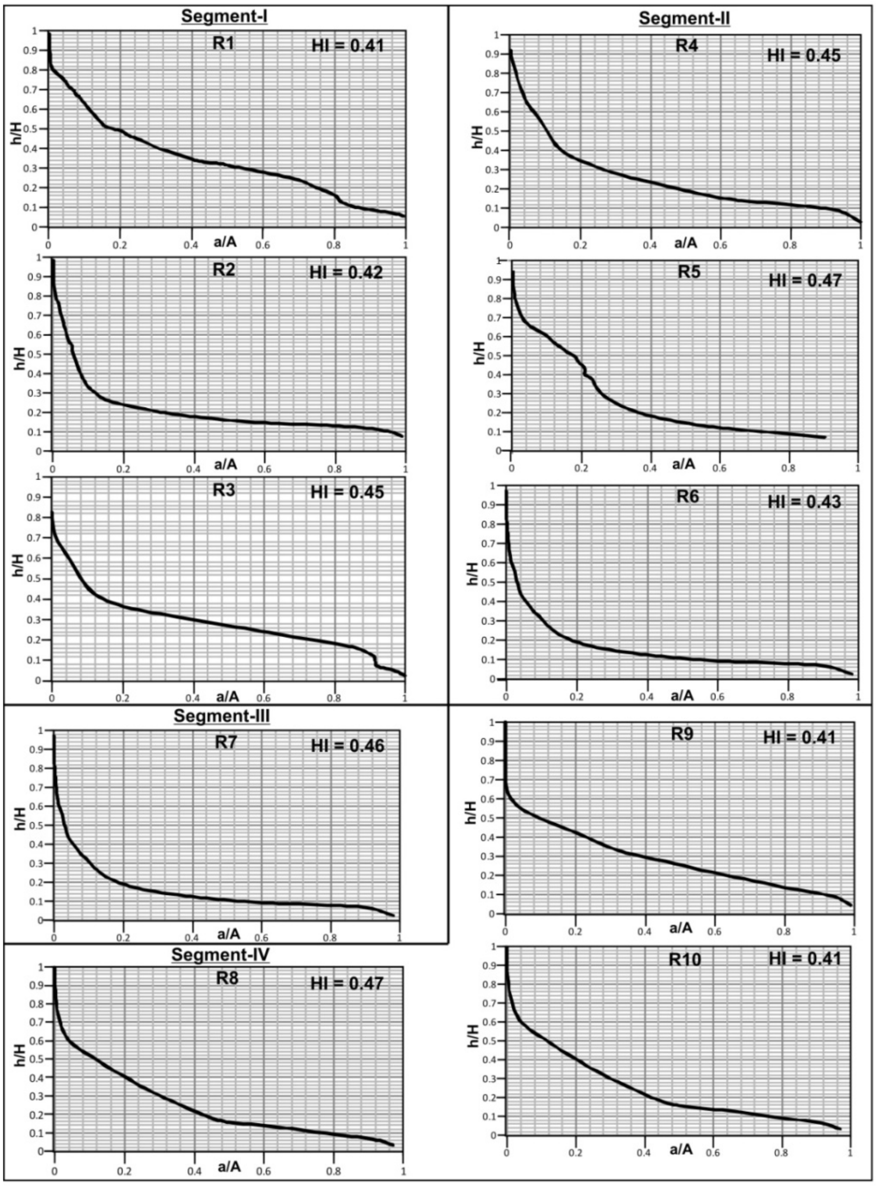

Figure 5.7 Hypsometric curves of the drainage basins (R1 to R10) traversing the NSF in the study area. The values of hypsometric integral are also shown.

Drainage basin asymmetry

The asymmetry factor (AF) is a rapid technique to evaluate the active ground tilting produced by tectonic activity or strong lithological control at drainage basin scale (Hare and Gardner, 1985; Keller and Pinter, 2002). It is defined as,

$$AF = 100 \, (A_r / A_t),$$

Where A_r, is the area of the basin to the right of the trunk stream (facing downstream), and A_t is the total drainage basin area.

An AF value of about 50 indicates tectonically stable landmass with uniform lithology (Dehbozorgi et al., 2010). AF values greater or less than 50 suggest tilting of the surface over which rivers are flowing. Perez-Pena et al. (2010) suggested that the magnitude of deviation of AF values from 50 is indicative of the degree of asymmetry. Deviation of 5 indicates symmetrical basins, whereas deviations of 5-10, 10-15 and >15 indicate gently asymmetrical, moderately asymmetrical and strongly asymmetrical basins respectively.

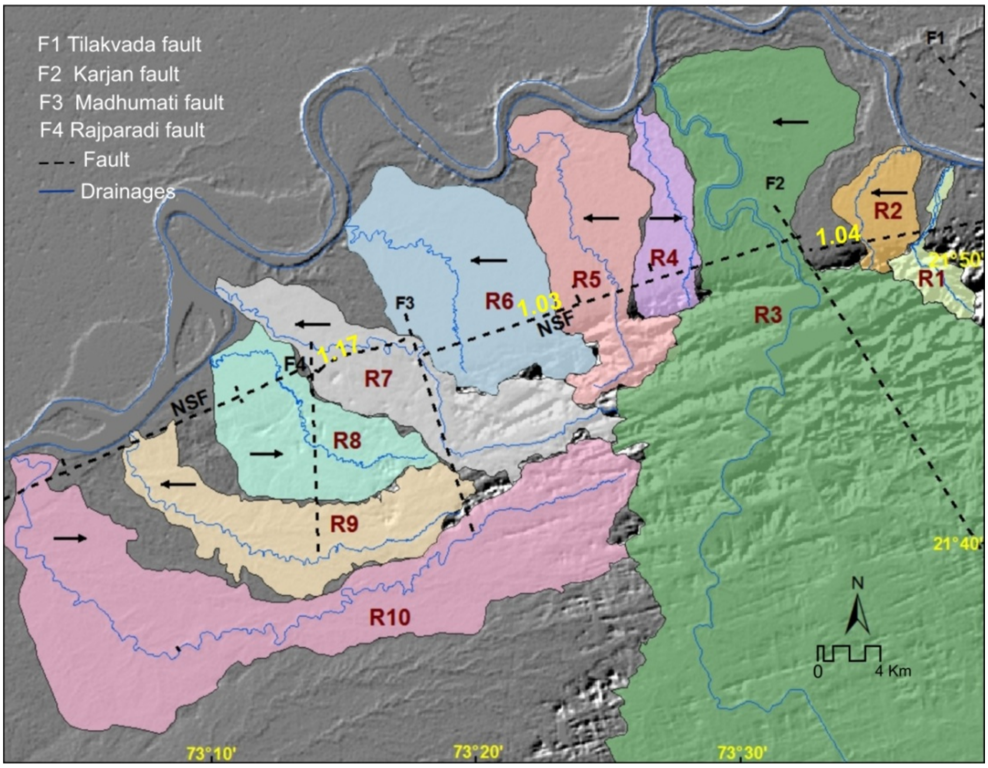

Figure 5.8 Map of showing drainage basins R1to R10 and the direction of tilting (indicated by black arrows) as revealed by drainage basin asymmetry. Note in segment-I, R2 & R3 shows westward tilting; in segment-II, R4 shows eastward tilting whereas R5 & R6 shows westward tilting; in segment-III, R7 shows westward tilting. This pattern correlates with the topographic profiles of the alluvial plain shown in Figure 9A. In segment-IV, R8 & R10 shows eastward tilting whereas, R9 shows westward tilting. This anomalous tilt pattern is attributed to complexly folded and faulted Tertiary rocks. Segments studied for mountain front sinuosity and the S_{mf} values obtained are also shown.

The AF values calculated for ten drainage basins of the study area, with arrows indicating inferred directions of ground tilting, are shown in Fig. 5.8. In the study area, there is a definite pattern in AF values. All drainage basins, except R1 (AF value 49), are moderately to strongly asymmetrical (Fig. 5.8). The variations in asymmetry, however, closely correlate with the segments of the NSF. In Segment I, the basin R1 is symmetrical (AF value is 49) which drains the easternmost part of the segment. The basins R2 and R3 are strongly asymmetrical (AF value is 76 and 71) suggesting tilting of the ground towards west (Fig. 5.8). In Segment II, R3 basin shows AF value 33 with suggested tilt direction towards east (Fig. 5.8). AF value of 58 for R5 basin located in the central part of this segment indicates gentle asymmetry while R6 basin (AF value is 75) is strongly asymmetrical with tilting in the same direction. Tilting in both east and west directions (Fig. 5.8) suggests gentle warping of the alluvial surface in Segment II concomitant with uplift due to neotectonic activity along the NSF. The warping is further corroborated by the slope directions of the topographic profile of this segment.

The transverse fault controlled R7 basin is the only basin that drains the Segment III. AF value of 57 for this basin suggests gently asymmetrical basin with suggested tilting towards west (Fig. 5.8). This is in continuity with westerly tilt at the margin of the segment II indicated by the strongly asymmetrical R6 basin. The R8, R9 and R10 basins, in segment IV, haven given AF values of 33, 60 and 39 respectively (Fig. 5.8). The R8 basin is strongly asymmetrical with suggested tilt of the ground towards east while the moderately asymmetric R9 basin indicates tilting towards west (Fig. 5.8). However, the strongly asymmetric R10 basin indicates ground tilting towards east. We attribute the abrupt changes in tilt directions of adjacent basins to the anomalous slopes developed over complexly deformed Tertiary rocks. The pattern of changes in the drainage asymmetry is found to correlate well with the segments of the NSF.

Stream Length gradient index (SL index)

The SL index was initially used to infer stream power and differential rock erodibility (Hack, 1973), since it is sensitive to minute changes in channel slope. In landscape evolution the adjustment of stream profile to tectonic activity is assumed to occur quickly which will be reflected by change in channel gradient. Therefore, the SL index is used to identify recent tectonic activity by looking for anomalous changes in index values on a particular rock type (Keller and Pinter, 2002; Merrits and Vincent, 1989, Brookfield, 1998, Chen et al., 2003, Zovoili et al., 2004; Troiani and Seta, 2008). Also, SL index is a valid tool for measuring perturbations along stream longitudinal profile (Burbank and Anderson, 2001) and has been successfully used as an indicator of uplifted zones (Merrits and Vincent, 1989; Chen et al., 2003; Harkins et a., 2005; Troiani and Seta, 2008, Font et al., 2010) and for detecting tectonic activity along particular channel segment (Azor et al., 2002, Chen et al., 2003, Zovoili et al., 2004,).

SL index analysis was performed for all the ten drainage basins in the study area using methodology described by Hack (1973), which is given as;

$$SL = (\Delta H / \Delta L)\, L$$

For a given segment of a river, SL is the stream length gradient index, $\Delta H/\Delta L$ is the channel slope or gradient of the reach and L is the total channel length from the midpoint of segment where the index is being calculated upstream to the highest point on the channel.

Since the prime objective of the present study is to investigate the neotectonic influences on the alluvial terrain, the SL analysis was carried out for the streams dissecting through the alluvial plain to the north of the range front scarps marking the NSF. For this, the trunk stream of each drainage basin was segmented at 10 m interval and SL index calculated from 100 m elevation to maintain uniformity of data along the length of the NSF zone (Table 5.1).

To recognize the relative magnitude of uplift within alluvial terrain, the SL index map was prepared in ArcGIS (Fig.5.9). To prepare index map, SL values were given to the midpoint of each channel segment of each drainage basin and the new field was added to the attribute table of the previously generated midpoint data. Subsequently, the calculated values were classified into four classes and SL index map prepared by contouring the midpoints having value that fall in the same class (Fig.5.9).

Segment I

In segment-I, the drainage basin R1 shows relatively high SL values throughout its alluvial reach with two prominent channel segments of 90-80 and 60-50 contour interval having anomalous high SL index value of class 3 (SL value: 100-500) (Table 5.1). The high SL index values coincide with the steep channel gradient developed within the alluvial reach (Fig.5.5) as seen on the longitudinal profile. In R2 basin, low SL index values of class-1 (10-50) and class-2 (50-100) is seen (Table 5.1). However, relatively high SL index values occur at the channel segment of 90-80 contour interval (SL value increases from 63.06 to 93.03) which coincide with the trap-alluvium contact, as seen on the longitudinal profile (Fig. 5.4, 5.9). Drainage basin R3, which forms the largest drainage basin of the segment, shows significant contrast in SL index values of trappean reach and alluvial reach. The channel segments of trappean reach are characterized by lowest SL index values of class 1 and 2 whereas within the alluvial reach they show the highest SL index values of class-5 (Table 5.1). The sudden increase in SL index value occurs at the channel segment of 90-80 contour interval and coincides with the trap to alluvium interface (Fig. 5.4, 5.9, 5.10). Overall, the drainages of segment I consistently show anomalously high SL index value at channel segment of 90-80 contour interval that coincides with the trap-alluvium interface that possibly represents the probable location of the NSF in the subsurface in front of the scarps.

Table 5.1 Stream Length gradient index (SL index) values calculated for the drainage basins of the study area.

Contour Interval	R1	R 2	R3	R4	R5	R6	R7	R8	R9	R10
240-250	244.60	113.3935	38.61	10	105.8637	-	10	-	-	28.155
230-240	645.28	117.0558	34.15	16.6342	47.5631	-	13.5431	-	-	27.7741
220-230	153.63	47.7691	40.33	24.0305	23.1309	-	13.8362	-	-	28.2812
210-220	105.75	89.5670	66.66	30.6018	53.5622	-	14.2844	-	-	22.6944
200-210	61.08	169.996	67.33	46.8488	40.0488	-	37.0355	-	-	30.4223
190-200	165.21	184.0124	48.79	120.7615	55.4486	-	70.7584	-	-	23.9303
180-190	81.35	199.5916	44.64	172.6272	54.2790	-	36.2204	-	-	28.1372
170-180	160.30	212.7136	48.70	166.8947	280.8810	-	35.6072	-	-	29.6472
160-170	88.17	246.5514	63.76	59.9684	74.9684	-	195.9141	-	-	29.1513
150-160	668.81	106.3064	93.02	51.3880	51.3880	-	65.8819	-	-	60.6557
140-150	116.88	78.9454	128.76	136.9161	235.4675	-	161.68995	-	26.7447	46.3368
130-140	238.37	60.3165	203	111.6889	158.9951	-	36.1954	-	22.5186	59.6364
120-130	83.63	210.8930	60.04	43.2079	191.3938	-	1866.7890	-	20.0326	52.1555
110-120	172.68	126.7073	144.67	55.2610	1426.0249	-	468.7991	-	15.7119	56.0405
110-100	171.35	46.3349	21314.18	55.5766	122.1521	-	81.4113	11.25	24.1768	47.3806
100-90	131.41	63.0676	6224.73	41.9371	1260.2169	17.0187	99.7942	15.94	32.7659	74.8489
90-80	164.48	93.3043	21145.84	69.2678	53.0040	23.5770	187.2431	28.25	23.5770	79.7578
80-70	100.52	49.2702	20513.98	53.8924	72.7287	20.1571	255.4469	39.97	26.2152	49.7977
70-60	114.86	37.9980	18167.68	92.1264	82.7728	28.0408	175.7922	39.97	31.8839	51.6391
60-50	141.00	39.3983	15625.74	46.3648	84.5393	18.0387	766.9181	44.45	42.1077	903.6895
50-40	110.92	38.1387	13925.74	67.3699	109.334	41.2959	1709.7094	37.53	48.7394	714.2763

Segment II

In the middle segment, drainage basin R4 shows low to intermediate SL index value of class 1, 2 and 3 (Table 5.1) throughout the reach. There are two channel segments of 90-80 and 50-40 contour interval within alluvial reach where sudden increase of SL index value is seen. The former high SL value coincides with the trap to alluvium transition and the later with steep channel gradient (Fig. 5.4, 5.9). Similarly, the drainage basin R5 shows two segments with anomalously high SL values of class 5 and class 3 occur at 100-90 and 50-40 contour interval respectively (Fig. 5.9, 5.10). The SL value of class 5 coincides with knick point located at the trap-alluvium contact and the second high value of class 3 overlap with the steep channel gradient within alluvium, visible on river longitudinal profile (Fig.5.9). R6 is the smallest drainage basin of the study area that shows low SL index values of class-1 throughout the reach (Table.5.1). However, relatively high SL index value is found to occur at contour interval 50-40 where it increases abruptly from 18.03 to 41.29. The increase in SL value coincides with steep convexity of longitudinal profile in alluvial reach (Fig. 5.9).

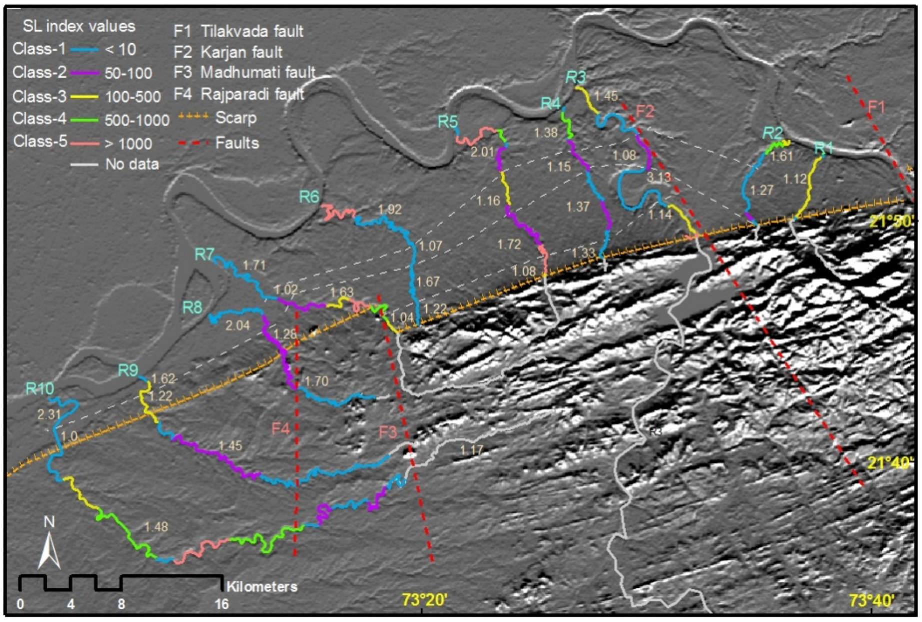

Figure 5.9 SL index map for drainage basins R1 to R10. Note the high SL values of class-3 & 5 in segment-I (R1 & R3), class- 3 in segment-II (R5), class- 3, 4 & 5 in segment-III (R7) in the vicinity of scarpline. Dashed lines demarcate different sinuosity zones delineated on the basis of variation in sinuosity pattern and sinuosity values. Note the zone of low sinuosity values correlating with the zone of high SL index values. On the contrary, zones of high sinuosity values are the zones of low SL index values.

All drainages of segment II consistently show high SL values in two channel segments at contour intervals 90-80 and 50-40 (Table 5.1). The first one is attributed to the trap-alluvium contact presumably coinciding with the NSF in the surface in front of the scarps, which correlates with similar change at the same contour level observed in segment I to the east (Fig. 5.9). The second one relates with the convex segments of the longitudinal profiles of the rivers and is attributed to increased incision in alluvium.

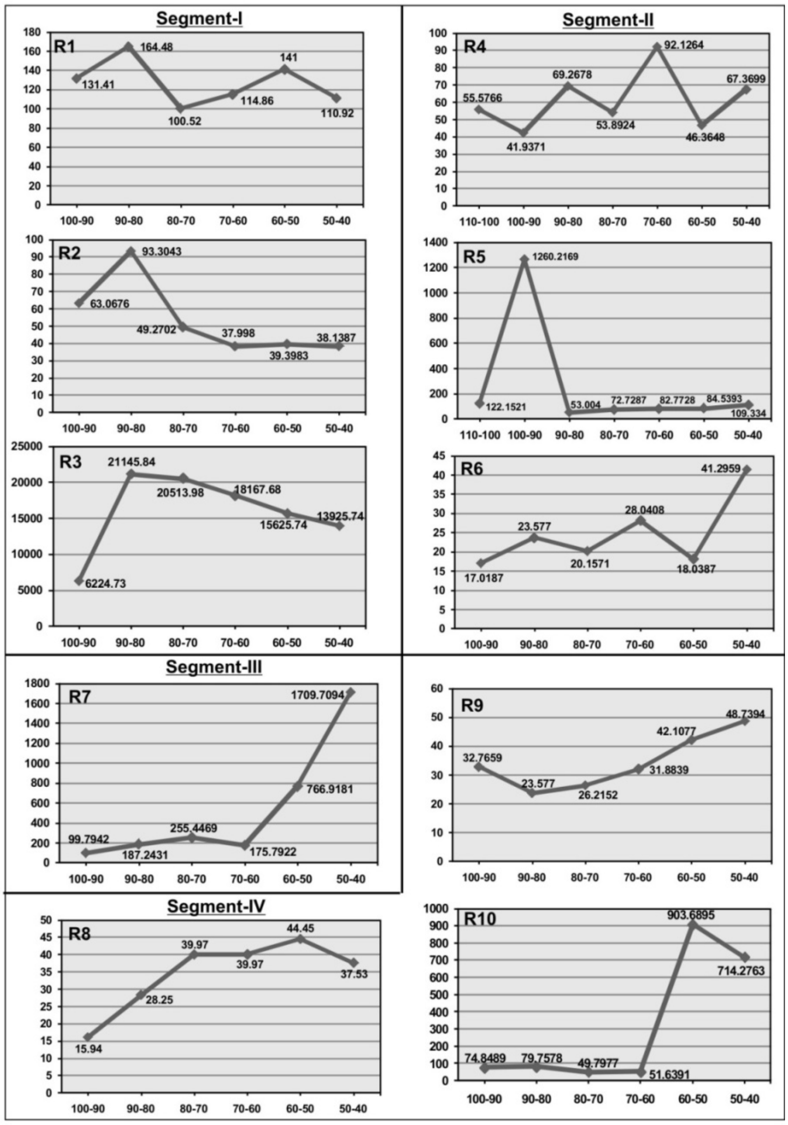

Figure 5.10 Graphs showing the variation pattern of SL- index values from upland to downstream direction. Contour values are plotted on the X-axis while the SL index is plotted on the Y-axis.

Segment III

In the R7 drainage basin channel segments of trappean reach show dominantly low to intermediate SL index values of class 1 and 2 which increases in the alluvial reach to class-3, 4 and 5 (Fig. 5.9). Within alluvial reach two distinct segments of high SL index value at contour interval 80-70 and 50-40 coincide with steep channel gradient (Fig. 5.9).

Segment IV

R8 is the smallest drainage basin of this segment and have low SL index values of class-1 (SL value: 10-50) through the entire reach (Fig. 5.9). Although, there is a gradual increase in SL index values from upper to lower reaches, an abrupt increase occurs at channel segment of 60-50 contour interval that coincides with the steep channel gradient of the river in Tertiary rocks (Fig. 5.9). A similar pattern of SL values is observed in case of basins R9 and R10 as well. The channel segments have, in general, low SL index values of class-1 (SL value: 10-50) throughout the reach. R10 is the largest drainage basin of this segment which shows low to high SL index values of class-1 and 4. Of this, the high SL values of class-4 are found within the narrow alluvial reach only.

The integrated analysis of SL index with longitudinal profiles has been carried out to infer the role of lithology and tectonic activity in producing the high SL values which has revealed that some of the high SL values are located at knick point and coinciding with NSF zone (trap to alluvium transition) while the other coincide with steep channel gradient in alluvium (Fig. 5.4). Further to understand the distribution pattern of SL index values within alluvial reach, SL graphs were prepared (Fig. 5.10).

Sinuosity

Sinuosity is an important parameter for the rivers located in tectonically active areas (Gomez et al., 1991; Keller and Pinter, 2002). It records the secondary effect related uplift by increasing or decreasing channel sinuosity. A river meanders when straight line slope of the valley is too steep to maintain the equilibrium between channel slope with discharge and sediment load because, the sinuous path of the meander reduces the slope of the channel and allowing river to maintain the equilibrium. This process creates a particular sinuosity pattern which can be evaluated by calculating channel sinuosity of identified channel segments (Adams, 1980). It is measured as;

$$\text{Sinuosity (S)} = \text{Channel length/Channel Valley} = C/V$$

All drainages in the study area show, highly sinuous channels in the alluvial plain that conform to their proximity with a major fault zone i.e. the NSF. However, visually observable variations in degree and pattern of sinuosity are seen along individual channels which have been used for subdividing the channels into specific reaches for sinuosity measurements.

In general, the sinuosity values are found to be on the higher side in all segments which indicates the influence of neotectonic activity. However, the sinuosity analysis reveal roughly E-W trending alternating zones of relatively high and low sinuosity in the alluvial terrain to the north of the NSF scarps as shown in Fig. 5.9. In segment I, two broad zones are formed, where the zone of relatively low sinuosity is closer to the scarpline whereas the higher sinuosity is closer to the Narmada River (Fig. 5.9). In segment II sinuosity based zonation is very clear (Fig. 5.9). Here, the narrow zone of lower sinuosity is near the scarpline. The lower sinuosity is because of the fact that all rivers follow a straight deeply incised channel for a short distance as they emerge from the trappean highland into the alluvial plain. This is followed by a zone of relatively high sinuosity towards north, the sinuosity decreases again before final zone of high sinuosity near the Narmada River is achieved. Interestingly, the two zones of low sinuosity correspond to the zones of high SL index in this segment, suggesting a strong but negative correlation between the sinuosity parameters and SL index (Fig. 5.9). This could be because of the tendency of rivers to flow straight in response to increase of gradient in downstream direction before adjusting and settling down to a stable sinuous course. In the segment-IV, in spite of the extremely narrow alluvial plain between the Tertiary uplands and the Narmada River, a zone of low sinuosity and a zone of high sinuosity is noted (Fig. 5.9).

INFERENCES

Geomorphic analysis

Tectonic activity along active faults exerts significant impact on geomorphologic properties of the landscape (Gordon, 1998; Gimboni et al. 2005). There have been many attempts to systematically investigate geomorphic response to tectonism with the help of several geomorphic indices in various tectonically active areas or fault zones such as central European southern Rhine graben (Gimboni et al. 2004a, 2005), the Normandy intraplate area of NW France (Font et al. 2010), Central Italy (Troiani et al. 2008), southwestern USA (Bull McFadden, 1977), the Pacific coast of Costa Rica (Wells et al., 1988), the Meditterranean coast of Spain (Silva et al., 2003), the Midcontinent of US (Adams, 1980), Ventura basin of southern California (Azor, 2002), Marrakech High Atlas (MHA) of Morocco (Delcaillau et al.,2010), Central Range Fault of Eastern Taiwan (Burce et al., 2006)…

The major geomorphic elements of the study area comprise the rugged uplands bounded by ENE-WSW trending scarps marking the NSF and the northward sloping alluvial plain. The area is drained by north flowing rivers that meet the Narmada River. The present remote sensing and GIS based study was carried out to understand the pattern of neotectonic activity along the NSF and related cross faults. DEM was analysed for understanding elevation related attributes of an area especially along the fault zone (Menges, 1990; Duncan et al., 2003). Conventionally, tonal variations in a DEM are interpreted as changes in elevation and the continuous linear high intensity tonal boundaries for long distances are associated with linear scarps or mountain fronts (Ganas et al., 2005).

The DEM confirms a continuous ENE-WSW trending dark yellow to brown tonal boundary that indicates the position of the NSF scarps (Fig. 4.1). Towards west, the same trend is found to continue as a dark green tone that shows the continuity of scarp over Tertiary rocks and the palaeobank as it further extension towards west (Fig. 4.1).

Abrupt change in slope as seen in the DEM corresponding to the NSF scarp line indicating active faulting (Fig. 5.1). This slope is found to have a value of 19.4 degrees. The other significant feature in the slope map is the high degree of slope of the alluvial surface in segment II in front (north) of the scarp (Fig. 5.1). This indicated that the slope is tectonically generated due to active faulting along the NSF. This is further complimented by the northward decreasing incision by the drainages. On the aspect map, the ENE-WSW trending scarpline is manifested by dark pink tone (Fig. 5.2). The northward flowing incised drainages also show dark pink tone (Fig. 5.2). The responsible factor for this is active tectonics observed in the vicinity of the fault. Therefore recent tectonic activity along NSF is identified as major factor in producing linear slope breaks and incised channels.

Mountain front sinuosity is a very effective parameter to differentiate tectonically active fronts with inactive fronts based on their degree of youthfulness (Bull and McFadden, 1977; Keller and Pinter, 2002). A tectonically active front typically shows less sinuosity whereas inactive mountain fronts are characterized by high sinuosity which is attributed to dominance of erosional processes over tectonic activity. The range bounding NSF scarps have yielded low S_{mf} values that classify the entire front as class I, the highest tectonic activity class as defined by Bull and McFadden (1977). The NSF scarp in segment I and II have Smf value of 1.04 and 1.03 respectively and therefore may be interpreted as the tectonically most active segments of the NSF (Fig. 5.7). The combined Smf value of 1.17 for segment III and IV in the western part also point towards a somewhat youthful nature of the NSF scarp, although slightly higher value may be attributed to the relatively softer Tertiary sedimentary rock that makes up the scarp in segment IV. Overall, continued active tectonics is inferred as the major factor in maintaining the youthful nature of the NSF scarp.

Pronounced variations in the longitudinal profiles of the trunk streams of drainage basin R1 to R10 are seen (Fig. 5.4). In segment I, the profile characteristics show steep gradients with several knick points in the upland reach, with graded but nevertheless steep profile in the alluvial part (Fig. 5.4). This conforms to the lower depth of incision (~6 m) in this segment. In the segment II the profiles of trunk streams R4-R7 show distinct convex up morphology in the alluvial reach that lies to the north of the NSF scarp. This also relates to the greatest depth of incision (~ 40 m) and to highest altitude of the alluvium in this segment. The long profile of Madhumati River is concave up in the alluvial reach (Fig. 5.4). It is the only river in the segment III but it does not flow strictly northward as mentioned above. The long profiles of the rivers in segment IV show convex up morphology for most part of their courses fall within the internally deformed Tertiary rocks which is attributed to neotectonic rejuvenation (Fig. 5.4). The steep gradient in the narrow alluvial rock at this downstream ends suggests neotectonically active nature of the NSF in this segment as well. The variable morphology of the long profiles spatially along the NSF is significant.

Hypsometric analysis was found useful for comparison of drainage basin of various sizes traversing the NSF zone. The convex up hypsometric curve indicate relatively young topography, S-shaped characterizes moderately eroded regions while concave curves indicate relatively old regions (Strahler, 1957; Delcaillau et al., 1998; Keller and Pinter, 2002). The hypsometric curve of the alluvial surfaces in the NSF zone show concave shapes in the first instance (Fig. 5.7). However a closer view shows the convex up tendency of the curves. This is clearly seen in curve of R1 in segment I, R5 in segment II and R9 in segment IV (Fig 5.7). The convex part coincides with the area in the close vicinity of the NSF indicating relatively young stage due to neotectonic rejuvenation of the NSF. The curves in conjunction with HI value suggest moderately eroded landscape of the study area. The mean value of HI is highest in segment II which confirms with the higher degree of tectonic activity indicated by other parameters (Fig. 5.7).

The drainage Asymmetry Factor (AF) is a good indicator of active ground tilting (Keller and Pinter, 2002; Dehbozorgi et al., 2010; Perez-Pena et al., 2010). AF value of the drainage basins astriding the NSF zone indicate ground tilting are shown in Fig. 5.8. All basins are moderately to strongly asymmetric and show a definite pattern in the variation of AF values that closely correspond to the morphology of the alluvial plain in different segments (Fig. 5.8). In segment I (R1-R3), the AF values suggest westward tilting. In segment II (R4-R6), eastward tilting in eastern part and westward tilting in the western part is suggested. This correlates with the physiography of the alluvial surfaces in this segment as shown in the topographic profile which matches with that of the uplands. Westward tilting indicated in segment III confirms to the westward and northward oriented course of the Madhumati River in the alluvial plain. The drainage basins of the segment IV show anomalous tilt direction as they mostly flow in the complexly deformed Tertiary rocks (Fig. 5.8). AF values of these basins could not be interpreted because of the extremely short alluvial reach of these rivers.

The SL index was calculated for the entire alluvial zone in part of NSF scarps. High SL index values were obtained consistently closer to the scarp between 90-80 m contour intervals in all the segments of the NSF (Fig. 5.9, 5.10). This coincides with the Trappean/Tertiary and Quaternary alluvial interfaces which presumably marks the actual fault line of the NSF in the subsurface (Fig. 5.4, 5.9). A second E-W trending zone of anomalously high SL index values occur at 60-50 m contour interval in segment I, between 50-40 m contour interval in segment II and segment III (Fig. 5.4, 5.9). This zone of the high SL values may be attributed to the distal end of the alluvial inferred from the contour pattern. In segment IV, high SL values are seen between 60-50 m contour intervals within the deformed Tertiary rocks (Fig. 5.4, 5.9, 5.10). However, high SL index values of class 4 in the narrow alluvial reach between the NSF scarp and the Narmada River suggest neotectonic activity along the NSF.

Variations in SL index values spatially along the NSF suggest varying intensity of neotectonic activity. Lithological control is ruled out as these variations are recorded in unconsolidated alluvial sediments that have homogeneous composition in all segments of the NSF zone. In segment I the SL index values in 90-80 m contour interval are 164.48, 93.30 and 21145.84 for R1, R2 and R3 basins respectively (Table. 5.1) (Fig. 5.9, 5.10). The highest value for R3 basin could be attributed to the Karjan Fault along which the Karjan River flows (Fig. 5.9). In segment II, the SL index values are 69.26, 1260.21, and 23.57 in R4, R5 and R6 basins respectively (Fig. 5.9). The SL index value of R5 basin correlates with the highest elevation attained by alluvial sediments in the entire length of the NSF zone. For R7 basin in segment III, the highest SL index value is 255.44 close to the scarp line which can be attributed to the Madhumati Fault that controls the basin (Fig. 5.9, 5.10). In segment IV the highest SL index values in the 50-40 m contour interval close to the NSF scarp are 44.45, 42.10 and 903.68 for R8, R9 and R10 basins respectively (Fig. 5.9, 5.10). Leaving the anomalously high SL index value of R3 basin (Karjan River basin), it is found that the segment II shows highest intensity of neotectonic activity followed by segment III, segment I and segment IV.

Perez-Pena et al. (2009) have explored the relation between graded river gradient (K), SL index and stream power (Ω) and confirmed that the SL index and K have the same formulation when applied to the whole river profile. To obtain K-Ω relation K and total stream power Ω_T for each river by applying the following equations:

$$K = C\text{-}.h_f / \ln L_t \qquad \text{(Perez-Pena et al., 2009)}$$

$$\Omega_T = \gamma Qs \qquad \text{(Summerfield, 1991)}$$

Where, C is the river head elevation, h_f is the elevation at the river mouth, L_t is the total length of river, γ is the unit weight of water per unit length (9800 N/m^3), Q is the discharge (m^3/s) and s is the slope of the water surface, which is generally approximated by the slope of the channel bed. Discharge Q calculated by applying the power law relation between the drainage area (A) and discharge (Q).

$Q = aA^b$ (Finlayson and Montgomery, 2003; Jain et al., 2006)

Where, a and b are the positive constants.

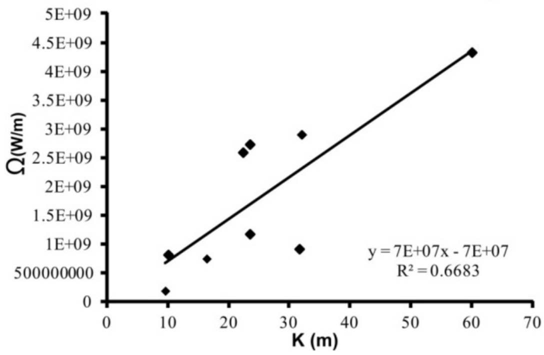

Figure 5.11 Graph showing the relationship between stream power (Ω) and graded river gradient index (K) for the drainage basins (R1-R10) of the study area.

These relationships imply that if drainage area increases A, the stream discharge Q, the graded river gradient K and stream **Ω** also increases. There is a linear correlation between graded river gradient K and total stream power Ω_T (Fig. 5.11). Because K represents the SL index of the entire river, it will correlate with the total stream power Ω_T. However, in case of the study area, small drainage basins also show high graded river index K, indicating a major role of neotectonics in generating such fluvial geomorphic anomalies.

Visual examination of the topographical maps and relative data reveal that the rivers in the study area have highly sinuous channels (Fig. 5.9). Sinuosity values calculated for the trunk streams of all the drainage basins of the NSF zone show interesting results. In general it is found that the sinuosity values are relatively lower closer to the scarps (Fig. 5.9). This is due to the short straight segments of the rivers as they emerge from the uplands and enter into the steeper slope over the alluvial terrain. We attribute this to the steeper slope over the alluvium generated by tectonic movement along the NSF. This confirms with the high SL index values discussed earlier. The highest sinuosity values are observed close to the Narmada River (Fig. 5.9). In segment II, four alternating E-W trending zone of relatively low and high sinuosity are observed. In segment III, three such zones are seen, whereas in segment I and IV, two such zones are formed (Fig. 5.9). Significantly, the low sinuosity zones correspond to the high SL index values whereas, the higher sinuosity zone correspond to the lower SL index values. We believe that the negative correlation between the sinuosity parameters and SL index is produced due to the tendency of the north flowing river to follow a straight course over steeper slopes, initially, before establishing the high sinuosity channels. The steeper north trending slopes were produced by neotectonic movements along the ENE-WSW trending NSF.

Pattern of neotectonic activity

Major transverse faults affecting the NSF have been delineated during the course of the present study. These include the Tilakwada Fault, Karjan Fault, Madhumati Fault and Rajparadi Fault. These cross faults divide the NSF in the study area into four morphotectonic segments from east to west. Close correspondence between the elevation of the alluvial plain to the scarp height and strong northward slope of the alluvial surface in various segments point towards a major role of tectonic reactivation of the NSF in the very recent past. The youthful nature of the mountain front scarp further corroborates the active nature of the NSF. The rivers flow along deeply incised and highly sinuous meandering channel all through their courses. All rivers show rapid decrease in incision away from the scarps suggesting an obvious control of neotectonic activity along the NSF on the incision. The depth of fluvial incision is also found to vary laterally along the length of the NSF.

Uplift of the alluvial plain with prominent tilting of the alluvial surface away from the NSF is attributed to differential uplift along the NSF where both the blocks, the southern block (upland) and the northern block (alluvium) present on either side of the fault have been uplifted. The various landscape parameters are found to vary spatially in the various segments along the NSF indicating variable magnitude of neotectonic activity in different segments. Lithological control is ruled out as the alluvial plain all along the NSF zone comprises unconsolidated fluvial sands, silts and gravel. The data presented in this study shows that maximum uplift of the alluvial plain occurred in segment II followed by segments III, I and IV. The variation in the depth of fluvial incision correlates with the morphotectonic segments delineated. In segment I maximum depth of incision is ~6 m while in segment II to the west it is of the order of ~40 m near the scarp. In segment III the maximum incision is ~ 15 m while in segment IV the incision is ~8 m. It is therefore, inferred that the NSF is characterized by vertical movements while the cross faults have undergone oblique slip movements leading to the development of morphotectonic zones with varying geomorphic characteristics.